# Zero loss magnetic metamaterials using powered active unit cells

**Yu Yuan, Bogdan-Ioan Popa, Steven A. Cummer**

*Center for Metamaterials and Integrated Plasmonics and Department of Electrical and Computer Engineering, Duke University, Durham, North Carolina, 27708*

*yuyuan.06@gmail.com, cummer@ee.duke.edu*

**Abstract:** We report the design and experimental measurement of a powered active magnetic metamaterial with tunable permeability. The unit cell is based on the combination of an embedded radiofrequency amplifier and a tunable phase shifter, which together control the response of the medium. The measurements show that a negative permeability metamaterial with zero loss or even gain can be achieved through an array of such metamaterial cells. This kind of active metamaterial can find use in applications that are performance limited due to material losses.



**OCIS codes:** (160.1245) Artificially engineered materials; (160.3918) Metamaterials; (350.4010) Other areas of optics : Microwaves

## References and links

1. J. B. Pendry,"Negative refraction makes a perfect lens," Phys. Rev. Lett. **85**, 3966 (2000).
2. S. Enoch, G. Tayeb, P. Sabouroux, N. Guerin, and P. Vincent, "A metamaterial for directive emission," Phys. Rev. Lett. **89**, 213902 (2002).
3. Y. Yuan, L. Shen, L. Ran, T. Jiang, J. Huangfu, and J. A. Kong, "Directive emission based on anisotropic metamaterials ," Phys. Rev. A **77**, 053821 (2008).
4. J. B. Pendry, D. Schurig, and D. R. Smith, "Controlling electromagnetic fields," Science **312**, 1780-1782 (2006).
5. D. Schurig, J. J. Mock, B. J. Justice, S. A. Cummer, J. B. Pendry, A. F. Starr, and D. R. Smith, "Metamaterial electromagnetic cloak at microwave frequencies," Science **314**, 977-980 (2006).
6. S. A. Cummer, B.-I. Popa, D. Schurig, D. R. Smith, and J. Pendry, "Full-wave simulations of electromagnetic cloaking structures," Phys. Rev. E **74**, 036621 (2006).
7. H. Chen, B.-I. Wu, B. Zhang, and J. A. Kong, "Electromagnetic wave interactions with a metamaterial cloak ," Phys. Rev. Lett. **99**, 063903 (2007).
8. S. A. Tretyakov, "Meta-materials with wideband negative permittivity and permeability," Microwave Opt. Technology Lett. **31**, 163-165 (2001).
9. A. D. Boardman, Y. G. Rapoport, N. King, and V. N. Malnev, "Creating stable gain in active metamaterials," J. Opt. Soc. Am. B 24, A53-A61 (2007).
10. R. R. A. Syms, L. Solymar, and I. R. Young, "Three-frequency parametric amplification in magneto-inductive ring resonators," Metamaterials **2**, 122-134 (2008).
11. A. Fang, Th. Koschny, M. Wegener, C. M. Soukoulis, "Self-consistent calculation of metamaterials with gain, " Phys. Rev. B **79**, 241104(R) (2009).
12. B. Nistad, and J. Skaar, "Causality and electromagnetic properties of active media," Phys. Rev. E **78**, 036603 (2008).
13. P. Kinsler, "Refractive index and wave vector in passive and active media," Phys. Rev. A **79**, 023839 (2009).
14. B. I. Popa and S. A. Cummer, "An architecture for active metamaterial particles and experimental validation at RF," Microwave Opt. Technology Lett. **49**, 2574-2577 (2007).
15. Y. Yuan, L. Ran, J. Huangfu, H. Chen, L. Shen, and J. A. Kong, "Experimental verification of zero order bandgap in a layered stack of left-handed and right-handed materials," Opt. Express **14**, 2220-2227 (2006).
16. H. Chen, J. Zhang, Y. Bai, Y. Luo, L. Ran, Q. Jiang, and J. A. Kong,"Experimental retrieval of the effective parameters of metamaterials based on a waveguide method," Opt. Express **14**, 12944-12949 (2006).
17. A. Sellier, S. N. Burokur, B. Kant, and A. de Lustrac,"Negative refractive index metamaterials using only metallic cut wires," Opt. Express **17**, 6301-6310 (2009).

#112519 - $15.00 USD Received 9 Jun 2009; revised 14 Aug 2009; accepted 21 Aug 2009; published 26 Aug 2009

18. O. Reynet and O. Acher, "Voltage controlled metamaterial," Appl. Phys. Lett. **84**, 1198-1200 (2004).
19. D. A. Powell, I. V. Shadrivov, Y. S. Kivshar, and M. V. Gorkunov, "Self-tuning mechanisms of nonlinear split-ring resonators ," Appl. Phys. Lett. **91**, 144107 (2007).
20. T. Hand and S. A. Cummer, "Characterization of tunable metamaterial elements using MEMS switches," IEEE Ant. Wireless Propagation Lett. **6**, 401-404 (2007).
21. D. Wang, L. Ran, H. Chen, M. Mu, J. A. Kong, and B.-I. Wu, "Active left-handed material collaborated with microwave varactors," Appl. Phys. Lett. **91**, 164101 (2007).
22. H.-T. Chen, W. J. Padilla1, J. M. O. Zide, A. C. Gossard, A. J. Taylor and R. D. Averitt, "Active terahertz metamaterial devices, Nature **444**, 597-600 (2006).
23. O. Paul, C. Imhof, B. Lgel, S. Wolff, J. Heinrich, S. Hfling, A. Forchel, R. Zengerle, R. Beigang, and M. Rahm, "Polarization-independent active metamaterial for high-frequency terahertz modulation," Opt. Express **17**, 819-827 (2009).
24. D. R. Smith, S. Schultz, P. Markos, and C. M. Soukoulis, "Determination of effective permittivity and permeability of metamaterials from reflection and transmission coefficients," Phys. Rev. B **65**, 195104 (2002).
25. X. Chen, T. M. Grzegorczyk, B. I. Wu, J. Pacheco, and J. A. Kong, "Robust method to retrieve the constitutive effective parameters of metamaterials," Phys. Rev. E **70**, 016608 (2004).
26. C. R. Simovski, and S. A. Tretyakov, "Local constitutive parameters of metamaterials from an effective-medium perspective," Phys. Rev. B **75**, 195111 (2007).
27. D. R. Smith, D. C. Vier, Th. Koschny, and C. M. Soukoulis, "Electromagnetic parameter retrieval from inhomogeneous metamaterials," Phys. Rev. E **71**, 036617 (2005).
28. U. K. Chettiar, A. V. Kildishev, H.-K. Yuan, W. Cai, S. Xiao, V. P. Drachev, and V. M. Shalaev, "Dual-band negative index metamaterial: double negative at 813 nm and single negative at 772 nm," Opt. Lett. **32**, 1671-1673 (2007).
29. T. Koschny, P. Markos, D. R. Smith, and C. M. Soukoulis, "Resonant and antiresonant frequency dependence of the effective parameters of metamaterials," Phys. Rev. E **68**, 065602(R) (2003).
30. M. V. Gorkunov, S. A. Gredeskul, I. V. Shadrivov, and Y. S. Kivshar, "Effect of microscopic disorder on magnetic properties of metamaterials," Phys. Rev. E **73**, 056605 (2006).
31. H. Chen, L. Ran, J. Huangfu, T. M. Grzegorczyk, and J. A. Kong, "Equivalent circuit model for left-handed metamaterials," J. Appl. Phys. **100**, 024915 (2006)
32. B.-I. Popa and S. A. Cummer, "Direct measurement of evanescent wave enhancement inside passive metamaterials," Phys. Rev. E **73**, 016617 (2006).

## 1. Introduction

Electromagnetic metamaterials are artificially engineered materials possessing highly versatile effective material properties. They offer the possibility of designing and building novel devices, such as perfect lenses that overcome the diffraction limit [1], directive antennas [2, 3] and invisibility cloaks [4, 6, 5, 7]. However, losses in metamaterials can severely limit their performance in these applications. It has long been recognized that powered active metamaterials can, in principle, be used compensate for metamaterial losses [8]. The theoretical challenges involved in creating stable active metamaterials are significant [9, 10]. Theoretical analysis has shown that complex behavior can result when gain elements are embedded in metamaterial structure [11], and the electromagnetic wave propagation, effective parameter characterization, and fundamental limitations resulting from causality related to the active metamaterials are also complex [12, 13]. Although initial experimental efforts have shown that the concept can be made to work [10, 14], active metamaterials have yet to be demonstrated in a realistic metamaterial configuration.

Here we report the fabrication and experimental measurement of a novel active magnetic metamaterial composed of arrays of unit cells designed based on the combination of an embedded radiofrequency (RF) amplifier and a tunable phase shifter, which together control the response of the medium. A basic architecture for powered active metamaterial particles was previously proposed and validated based on a single unit cell measurements [14]. Several significant improvements have been implemented in the work reported here. Like other metamaterials and their related physical properties in the RF domain [15, 16, 17], this kind of active metamaterial can be designed, fabricated, and find their applications in the terahertz or even higher frequency ranges.

#112519 - $15.00 USD Received 9 Jun 2009; revised 14 Aug 2009; accepted 21 Aug 2009; published 26 Aug 2009

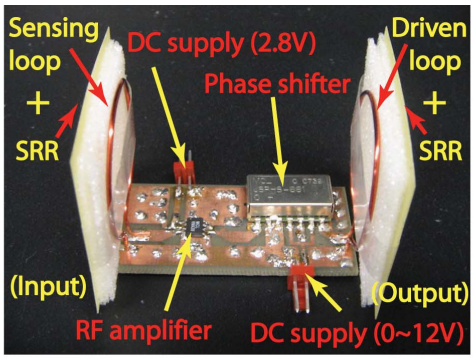


(a)

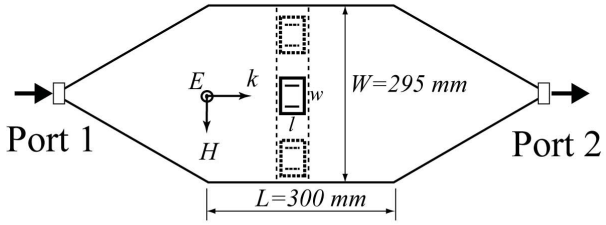


(b)

Fig. 1. (Color online) (a) Photograph of the constructed unit cell for the powered active magnetic metamaterial with individual components labeled. (b) A schematic of a single unit cell (solid) and three unit cells (dashed) inside the waveguide in the measurements. The incident magnetic field is perpendicular to the planes containing the loops, and volume under test to which all extracted effective parameters apply is bounded by the dashed lines.

## 2. Principle

In order to demonstrate the principle behind our tunable active magnetic metamaterial, descriptions of the magnetic moment of the unit cell and the resulting effective permeability are demonstrated as follows. In a medium for which the homogenization theory applies the constitutive equation that relates the magnetic field, **B**, and the **H**-field is, in the absence of magneto-electric coupling:

$$\mathbf{B} = \mu_0(\mathbf{H} + \mathbf{M}) \tag{1}$$

where **M** is the magnetization vector. The relative permeability tensor can be determined from this equation taking into account that $\mathbf{B} = \mu_0 \bar{\bar{\mu}}_r \mathbf{H}$. If **B**, **H**, and **M** are colinear, as is the case in our analysis, only one component of the permeability tensor is relevant and is given by

$$\mu_r = 1 + \frac{M}{H} = 1 + \frac{|M|\, e^{i\varphi}}{H}, \tag{2}$$

where the magnetisation $M$, i.e. magnetic moment per unit volume created in response to the external $H$-field, is written in the form $M = |M|\, e^{i\varphi}$, where the phase $\varphi$ is the phase of the magnetisation relative to the applied $H$-field. As noted in [14] controlling this phase enables direct control of the real and imaginary parts of the permeability. Our design exploits this observation. Following the architecture proposed in [14], our unit cell design comprises basic components

#112519 - $15.00 USD Received 9 Jun 2009; revised 14 Aug 2009; accepted 21 Aug 2009; published 26 Aug 2009

such as a loop that senses the incident magnetic field, an amplifier that boosts the sensed signal, and a driven loop that creates the required magnetisation vector (see Eq. 2). In addition to these elements, several significant improvements have been employed to obtain a more practical design.

First, surface mount amplifiers are used to embed the gain elements inside the metamaterial unit cells. Second, two passive split ring resonators (SRRs) are placed adjacent to the sensing and driven loops to significantly enhance the local magnetic fields near the SRR resonant frequencies and thus reduce the active gain required for a strong material response. Finally, a voltage controlled phase shifter is placed at the output of the amplifier to control the phase at the drieven loop, which tunes the response of the cell.

This tunable element operates in a fundamentally different way than previously reported passive tunable metamaterials in which the tunable element controls the self resonant frequency or quality factor of the cell [18, 19, 20, 21, 22, 23]. Here the phase shifter directly tunes the relative phase between the magnetic field through the sensing loop and the magnetic dipole moment produced by the driven loop. This controls the phase of the complex magnetic susceptibility, i.e. the $\varphi$ term in Eq. (2), and therefore the real and imaginary parts of the effective permeability. This tunability proves important in creating a metamaterial with zero magnetic loss.

## 3. Realization and parameter characterization

A photograph of a unit cell is shown in Fig. 1(a). The sensing and driven parts consist of a 36 mm diameter copper loop and a SRR that is loaded with a 1 pF capacitor, resonant near 562 MHz, which is within the operation bandwidth of the RF amplifier. There are 3 mm-thick foam layers with a permittivity close to unity between the loop and the SRR that control the coupling between the loop and the SRR. Like typical passive metallic metamaterials, the unit cell volume is almost entirely air.

The sensing and driven loops are mounted on an FR4 circuit board, on which a Minicircuits VNA-28 monolithic RF amplifier and a Minicircuits JSPHS-661+ voltage controlled phase shifter are mounted. The RF amplifier is supplied with a 2.8V DC voltage, and a DC voltage range of 0 to 12V is applied to the phase shifter with a resulting phase shift of 0 to 220 degrees. The all dimensions of the unit cell are $w$ = 60 mm, $h$ = 50 mm, and $l$ = 40 mm, where $w$ and $h$ are the width and the height (both transverse to the direction of the wave propagation), $l$ is the length (along the wave propagation direction), and they are about 1/8, 1/10, and 1/12 of a free space wavelength around the operating frequency, respectively.

We should note that, as in [14], Eq. (2) can be expanded based on the geometry discussed above in order to obtain an acurate prediction of the effective $\mu_r$ of a bulk medium made of our active unit cells. However, such quantitative calculations are beyond the scope of this paper and provide little additional insight into how the cell behaves. Instead we use a well established experimental method to recover the effective permeability of the fabricated cells.

More specifically, Fig. 1(b) shows a schematic of a single unit cell and three unit cells placed in the waveguide, which is connected to an HP 8720A vector network analyzer. The procedure described in [24, 27, 25] was used to retrieve the effective permittivity and permeability from the measured S parameters. Note that both the one and three cell measurements are performed with TEM waves that fill the entire cross section of the waveguide. This means that the volume to which the extracted effective electromagnetic parameters apply is the same in each case, as denoted by the dashed lines in the figure.

It should be stressed that retrieval of effective electromagnetic (EM) parameters using a monolayer structure along the wave propagation direction has been well validated by previous research. For example, Chen *et al.* [25] showed that the retrieved impedances for one, two,

#112519 - $15.00 USD Received 9 Jun 2009; revised 14 Aug 2009; accepted 21 Aug 2009; published 26 Aug 2009

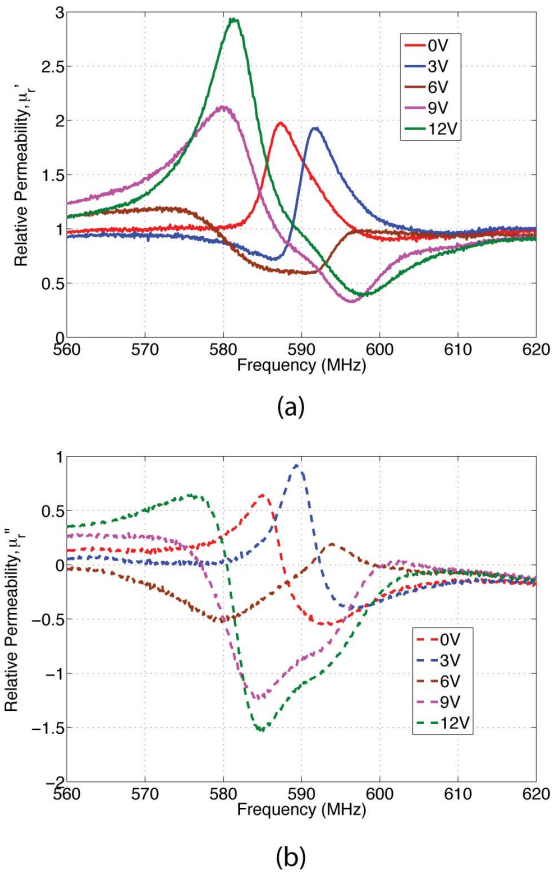


Fig. 2. (Color online) The subset of retrieved permeabilities (measured) for the unit cell: (a) the real part, and (b) the imaginary part.

and three cells of metamaterial match well for most frequencies, indicating that the impedance is independent of the slab thickness. In [26], the authors also conclude that one can attribute the EM parameters found for finite slabs and even for monolayer slabs to infinite lattices. As pointed out in the past, the obtained effective material parameters are non-local (i.e. they depend on the fields inside the whole medium) [26, 27]. Since only non-local parameters are currently available in experiments and have been measured in essentially all previous experimental metamaterials papers, we also compute only the non-local parameters in order to compare our results with past measurements.

The one and three cell configurations are equivalent to a metamaterial in which the number of unit cells per free space wavelength is in the transverse direction is 1.7 and 4.6, respectively. An individual cell is significantly subwavelength in size in all three dimensions, as noted above. Particularly for a single cell, the effective transverse spacing is large enough that the extracted parameters will apply only for normal incidence, as is the case for the majority of optical wavelength metamaterials that have been fabricated (e.g., [28]). With few cells per wavelength, diffraction could influence the reflection and transmission properties of the array. However, as shown below, the measured material parameters for the one and three cell configurations are completely consistent, indicating that diffraction effects are not playing a significant role.

#112519 - $15.00 USD Received 9 Jun 2009; revised 14 Aug 2009; accepted 21 Aug 2009; published 26 Aug 2009

The biasing network of the medium is composed of twisted-pair wire and surface mount shunt capacitors on the circuit board that serve to decouple the RF and DC parts in the medium. The wire pairs are also aligned perpendicular to the incident RF electric field to minimize any interaction with the biasing network. These minimize any impact of the biasing network on the effective medium parameters.

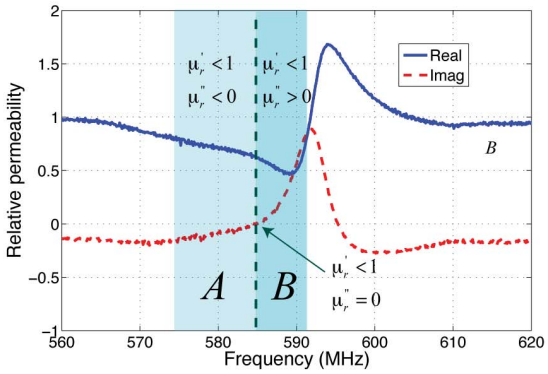


(a)

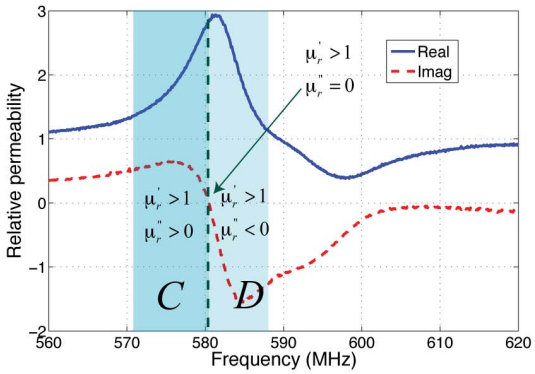


(b)

Fig. 3. (Color online) The retrieved permeability for the two cases: (a) $V_b = 4.5V$, and (b) $V_b = 12V$, where $V_b$ is the DC voltage supply on the phase shifter.

## 4. Measured EM parameters and their special features

In the measurement, the DC bias voltage ($V_b$) on the phase shifter ranged from 0V to 12V, with a step of 1.5V (9 states available for the active unit cell). A subset of retrieved permeabilities for various phase shifter biases are shown in Fig. 2. At all bias values, the unit cell exhibits a significant magnetic response slightly above the self resonant frequency of the passive SRRs due to the coupling between the SRR and the metallic loop. In each case the magnitude of the susceptibility is essentially resonant, falling as frequency moves away from a single maximum. Passive metamaterials allow only one susceptibility phase distribution, resulting in losses at all frequencies. In contrast, the combination of the amplifier and the phase shifter enable control

#112519 - $15.00 USD Received 9 Jun 2009; revised 14 Aug 2009; accepted 21 Aug 2009; published 26 Aug 2009

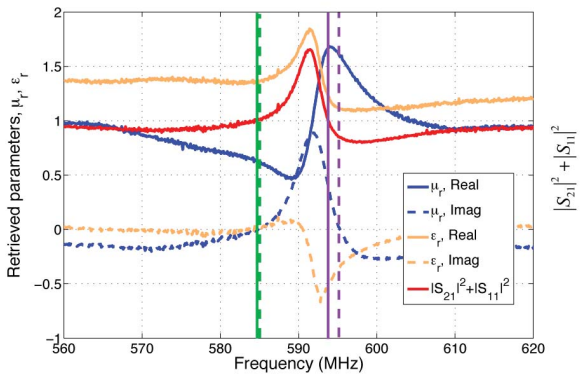


Fig. 4. (Color online) The retrieved permeability, permittivity, and the calculated total power loss in the case of $V_b = 4.5V$. Dashed lines denote the zero-imaginary-permeability frequencies, and solid lines denote the frequencies at which the unit cell is lossless.

over the relative phase of the current in the output loop with respect to the input voltage (and thus the applied magnetic field), and this clearly changes the magnetic response. For example, at the lower bias voltages, the magnetic response is predominantly positive ($\mu_r' > 1$) with some frequencies exhibiting loss ($\mu_r'' < 0$) and others gain ($\mu_r'' > 0$). As $V_b$ increases, the real permeability exhibits a bandwidth of strong negative response and the character of the imaginary permeability changes as well.

To demonstrate the specific ways in which the magnetic response of this particle can be controlled, two phase shifter bias voltages, $V_b = 4.5$ V and $V_b = 12$ V, are examined in detail in Fig. 3. All combinations of real and imaginary magnetic susceptibility signs are obtained: (A) $\mu_r' < 1$ and $\mu_r'' < 0$, (B) $\mu_r' < 1$ and $\mu_r'' > 0$, (C) $\mu_r' > 1$ and $\mu_r'' > 0$, and (D) $\mu_r' > 1$ and $\mu_r'' < 0$. The zero magnetic loss frequencies where $\mu_r' < 1$ and $\mu_r'' = 0$ and $\mu_r' > 1$ and $\mu_r'' = 0$ (as shown in Fig. 3(b)) are denoted by dashed lines. The case of $\mu_r' < 1$ and $\mu_r'' = 0$ is particularly interesting, for it can be used to realize negative permeability with zero loss from arrays of such unit cells, as demonstrated later in the paper.

For an active magnetic metamaterial, the frequency of zero imaginary permeability does not always align with the frequency at which the material is lossless because of the unavoidable electric response of the material [29]. However, the electric response of our fabricated cell is modest and does not strongly impact the overall material properties of this active unit cell. With $V_b = 4.5$ V as an example, the retrieved permeability, permittivity, and the total power emitted by the unit cell, defined as the sum of the transmitted and reflected power $|S_{21}|^2 + |S_{11}|^2$, are shown in Fig. 4.

In Fig. 4, there are two frequencies (585 MHz and 595.3) at which $\mu_r'' = 0$. At the first, the electric antiresonance has little effect, and the imaginary part of permittivity is zero, resulting in a material that not only has zero magnetic loss but also zero total loss. At the second, the effective electric response of the cell is significant and exhibits a negative imaginary permittivity. This results in a material that is magnetically lossless but not lossless overall.

The positive imaginary permeability measured in our powered magnetic metamaterial is completely distinct from that observed in passive electric metamaterials [29]. The latter occurs as a consequence of the non-locality of the extracted parameters and is not a true magnetic response in the sense that such an electric metamaterial will not respond to an applied magnetic field alone. In our case, the particles are excited directly by the magnetic field, which means that the positive imaginary permeability is a measure of the achieved magnetic gain.

#112519 - $15.00 USD Received 9 Jun 2009; revised 14 Aug 2009; accepted 21 Aug 2009; published 26 Aug 2009

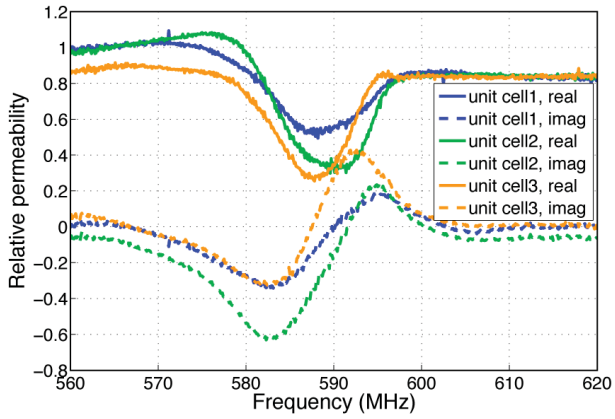


(a)

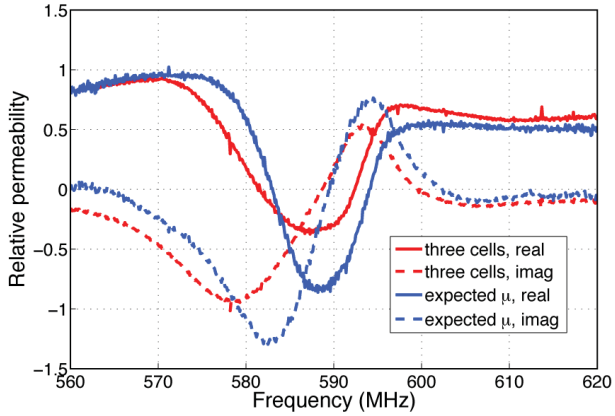


(b)

Fig. 5. (Color online) Retrieved permeability for (a) the three unit cells measured individually, and (b) an array of these three cells. Expected permeability from susceptibility adding of the individually measured unit cells is also shown in (b) for comparison.

This observation is supported by Fig. 4, that shows $|S_{11}|^2 + |S_{11}|^2 > 1$ in the bandwidth where $Im(\mu_r) > 0$.

To demonstrate that a metamaterial medium can be constructed by combining multiple elements, we measured an array of three identical unit cells. The three cells were first measured separately, each biased with $V_b \approx 6$ V for a strong negative permeability response with some fine tuning to make the response of each cell approximately identical (Fig. 5(a)). The three cells were then all placed in the waveguide with a spacing of 52 mm between the cells in the transverse direction (see the dashed lines in Fig. 1(b)).

The multicell array (Fig. 5(b)) exhibits a negative real permeability from 581.5 to 592.4 MHz. Over this frequency range, the imaginary part of the permeability changes from negative to positive, crossing zero at 588.7 MHz and giving zero total loss at 587.2 MHz. This shows

#112519 - $15.00 USD Received 9 Jun 2009; revised 14 Aug 2009; accepted 21 Aug 2009; published 26 Aug 2009

that this multicell metamaterial array realizes a negative permeability with either zero magnetic loss or zero total loss, depending on the specific frequency.

Figure 5(b) also shows the expected permeability if the magnetic susceptibilities measured from each individual cell simply add. Simple addition of the magnetic susceptibilities of individual particles will occur when the particles are electrically small, are minimally interacting, and are embedded in the same volume under test, as they are for our measurements. That the measured three cell permeability agrees closely with the simple added susceptibility permeability indicates the coupling between the closely spaced active cells is modest and the proximity of other cells does not significantly change the response of a single cell. The small discrepancy might be due to the mutual coupling between cells [30, 31], the effect of microscopic disorder [30] arising from the complex structure on the magnetic properties, or small changes, such as the cell configuration and the position, when the cell was measured separately and when it was put in an array. This shows that cells of this architecture can be assembled into larger arrays and thus larger metamaterial samples. When cells exhibit gain at certain frequencies there will be limits on how they can be assembled into medium that is stable and does not spontaneously oscillate [9]. We note that we have found that intercell coupling in similar active cells without a phase shifter can be difficult to control. The phase shifter in the unit cell has stable 50 ohm input and output impedance, and thus acts as a buffer to diminish the feedback from the output loop back through the amplifier.

## 5. Conclusion

In conclusion, we designed, fabricated and characterized a powered active magnetic metamaterial with tunable permeability. A negative permeability metamaterial with zero loss or even gain can be achieved through an array of such metamaterial cells. This kind of active metamaterial can find use in applications that are performance limited due to material losses, such as antennas based on magnetic metamaterials [3] or evanescent wave enhancement [32], and also points a way towards active metamaterials at higher frequencies where losses are more severe.

#112519 - $15.00 USD Received 9 Jun 2009; revised 14 Aug 2009; accepted 21 Aug 2009; published 26 Aug 2009